

5-29-2012

Size Dependent Antimicrobial Properties of Sugar Encapsulated Gold Nanoparticles

Lakshmisri Manisha Vangala

Western Kentucky University, lakshmisri.vangala672@topper.wku.edu

Follow this and additional works at: <http://digitalcommons.wku.edu/theses>

 Part of the [Medicinal-Pharmaceutical Chemistry Commons](#)

Recommended Citation

Vangala, Lakshmisri Manisha, "Size Dependent Antimicrobial Properties of Sugar Encapsulated Gold Nanoparticles" (2012). *Masters Theses & Specialist Projects*. Paper 1166.
<http://digitalcommons.wku.edu/theses/1166>

This Thesis is brought to you for free and open access by TopSCHOLAR®. It has been accepted for inclusion in Masters Theses & Specialist Projects by an authorized administrator of TopSCHOLAR®. For more information, please contact topscholar@wku.edu.

SIZE DEPENDENT ANTIMICROBIAL PROPERTIES OF SUGAR ENCAPSULATED
GOLD NANOPARTICLES

A Thesis
Presented to
The Faculty of the Department of Chemistry
Western Kentucky University
Bowling Green, Kentucky

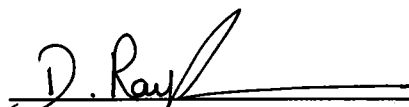
In Partial Fulfillment
Of the Requirements for the Degree
Master of Science

By
Lakshmisri Manisha Vangala


May 2012

SIZE DEPENDENT ANTIMICROBIAL PROPERTIES OF SUGAR ENCAPSULATED
GOLD NANOPARTICLES

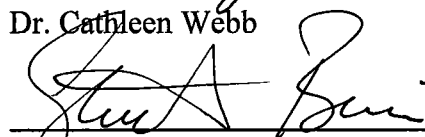
Date Recommended 5/11/2012



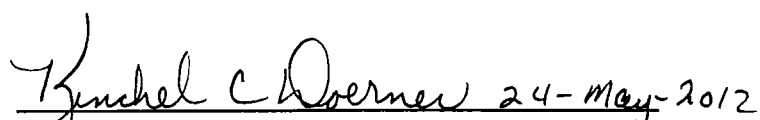
Dr. Rajalingam Dakshinamurthy,
Director of Thesis



Dr. Cathleen Webb



Dr. Stuart Burris



Dean, Graduate Studies and Research Date

ACKNOWLEDGMENTS

I would like to express my greatest gratitude to the people who have helped and supported me throughout my Masters. First and foremost, I would like to thank God almighty who has guided me throughout this journey. I am grateful to my research advisor Dr.Rajalingam Dakshinamurthy for his continuous support, knowledge and encouragement from beginning to this day. I attribute the level of my master's degree to his encouragement and effort, without whom this thesis would not have been completed.

I would also like to thank Dr. Cathleen Webb, Department Head, and Dr. Stuart Burris my committee members. They have been constantly helpful and I sincerely appreciate it.

To Dr. Andersland who was always willing to help and patiently answer all of my questions regarding microscopy.

A special thanks of mine goes to my colleagues/ friends Vivek, Shrikanth, Meghana, Sumit, Dillon, Matt, Jane, Helen and Chad who helped me in completing the project and exchanged their interesting ideas, thoughts and made this project easy and accurate.

I would like to thank all the faculty and staff of the Department of Chemistry for their support in my graduate career at Western Kentucky University.

Finally, I dedicate my thesis to my family; Mr. Satyakumar Vangala, Mrs. Latha Vangala, Miss Lakshmisri Manasa Vangala, Narasimha Manideep Vangala and Mr. Charan Dadigela who were always there whenever I needed and showed undivided support and interest which inspired me and encouraged me to go my own way. Without them I would have been unable to complete my project. Thank you one and all.

TABLE OF CONTENTS

1. Introduction	1
2. Materials and Methods	9
3. Results and Discussion.....	13
4. Conclusion.....	34
5. Future Studies.....	35
6. References	36

LIST OF FIGURES

1. Scale for Nanoparticles.....	1
2. Applications of nanotechnology	3
3. Comparison of the Gram positive and Gram negative bacterial cell walls	6
4. Reaction scheme showing the acetylation mechanism of alcohols.....	13
5. TEM images of dGNPs.....	15
6. Digital images showing Benedict's test.....	16
7. Images of acid-base titration.....	16
8. Turbidimetry graphs	19
9. Spreading plates and plots for <i>E. coli</i> against dGNPs/ Kanamycin.....	21
10. Agar diffusion plates and plot for <i>E. coli</i> against dGNPs/ Kanamycin.....	23
11. dGNPs induced disruption of <i>E. coli</i> cells	26
12. Propidun Iodide experiment for <i>E. coli</i>	28
13. Spreading plates and plots for <i>S. epidermidis</i> against dGNPs / Kanamycin.....	30
14. Propidun Iodide experiment for <i>S. epidermidis</i>	32
15. dGNPs induced disruption of <i>S. epidermidis</i> cells	33

LIST OF TABLES

1. Representing concentrations of dGNPs of three different sizes used to treat bacteria.....	23
---	----

SIZE DEPENDENT ANTIMICROBIAL PROPERTIES OF SUGAR ENCAPSULATED
GOLD NANOPARTICLES

Lakshmisri Manisha Vangala

May 2012

40 Pages

Directed by: Dr. Rajalingam Dakshinamurthy, Dr. Cathleen Webb and Dr. Stuart Burris

Department of Chemistry

Western Kentucky University

The antimicrobial properties of dextrose encapsulated gold nanoparticles (dGNPs) with average diameters of 25 nm, 60 nm, and 120 nm (± 5 nm) synthesized by green chemistry principles were investigated against both Gram-negative and Gram-positive bacteria. Studies were performed involving the effect of the dGNPs on the growth, morphology and the ultrastructural properties of bacteria. dGNPs were found to have significant dose dependent antibacterial activity which was directly proportional to their size and also their concentration. The microbial assays revealed the dGNPs to be bacteriostatic as well as bactericidal. The dGNPs exhibited their bactericidal action through the disruption of the bacterial cell membrane causing leakage of cytoplasmic content. The overall outcomes of this study suggest that dGNPs hold promise as a potent antimicrobial agent against a wide range of disease causing bacteria and can control and prevent possible infections or diseases.

INTRODUCTION

Definitions of nanotechnology are as diverse as the applications that are available. It can be defined as the ability to design and control the structure of an object at all length scales from the atom up to macro scale. The particles ranging from 10-100 nm are known as nanoparticles (Figure 1).¹ One of the reasons for the unique qualities of nanoparticles is the very small size of the materials.

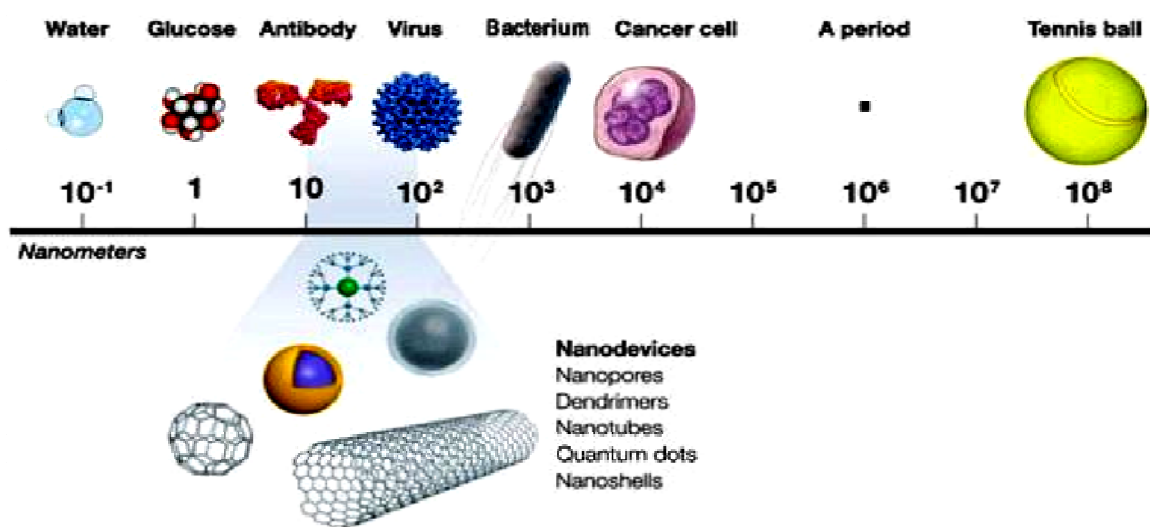


Figure 1: Scale for the comparison of Nanoparticles size.

At the nanoscale, many common materials exhibit unusual properties, such as lower resistance to electricity, lower melting points or faster chemical reactions. One such metal is gold (Au) which at the macroscale is shiny and yellow. Gold nanoparticles appear red in color when they are made to a size of 25 nm.² These smaller particles interact differently with light, so at each size range they appear in a different color. Depending on the size and shape of the particles, gold can appear red, yellow, or blue³. Gold nanoparticles may lead to new solutions to many of the problems the world is facing.

Nanoparticles are more reactive because they have more surface area than macroscale particles.

Today nanoparticle research is currently an area of intense scientific interest due to a wide variety of potential applications in biomedical, optical and electronic fields (Figure 2). GNPs are currently being used as a drug to cure various diseases, including certain life threatening diseases like cancer, Alzheimer's disease, etc. Some of the applications of nanoparticles in the field of biology/ medicine include:⁴⁻⁷

- Fluorescent biological labels
- Drug and gene delivery
- Bio-detection of pathogens
- Detection of proteins
- Tissue engineering
- MRI contrast enhancement
- Tumor destruction
- Antimicrobial agents

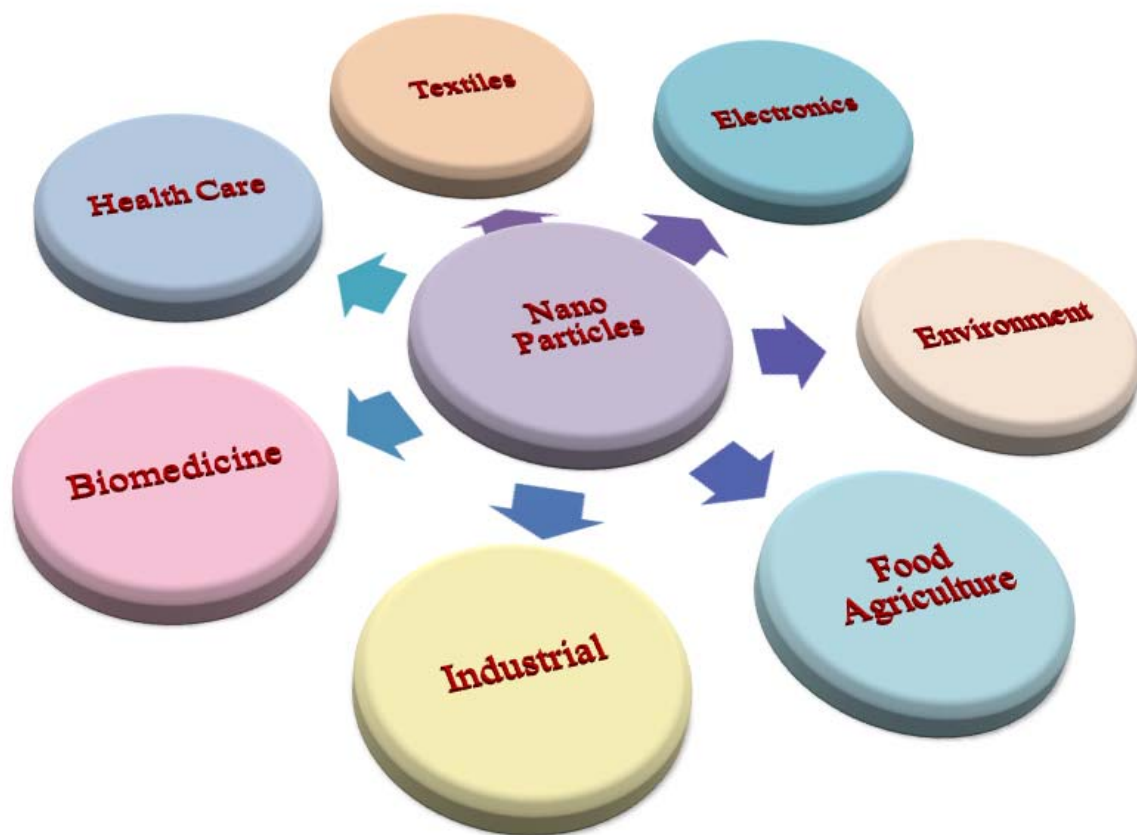


Figure 2: Schematic representation showing various applications of nanotechnology. Among all the applications, most of the applications affect the environment and human body. Hence, there is a need for environmentally friendly approach towards nanotechnology.

Multidrug-resistant (MDR) bacteria represent a major threat to the success of many branches of medical sciences. Some patients are especially vulnerable of acquiring MDR bacterial infections as a consequence of treatments for illnesses such as organ transplant, hemodialysis and various types of cancer.⁸ Each year at least 150,000 people die around the world due to the infection of a particular MDR bacterium.⁹ Therefore, there is an immense need for new strategies to design antibacterial agents.¹⁰ Depending upon the nature of the cell wall, bacteria are divided into two types:

- Gram Positive
- Gram Negative

The basic differences between the gram-negative and gram-positive bacteria are that: Gram-negative have a cell wall that does not retain crystal violet dye, whereas, the gram-positive organisms have a cell wall that retains the stain. The structure, components, and functions of the cell wall distinguish Gram positive from Gram negative bacteria (Figure 3).

Gram Positive Bacteria:

A Gram positive bacterium has a thick, multilayered cell wall consisting mainly of peptidoglycan (150 to 500 °A), surrounding the cytoplasmic membrane. The peptidoglycan is a meshlike exoskeleton similar in function to the exoskeleton of an insect. The peptidoglycan is essential for the structure, for replication, and for survival in the normally hostile conditions in which bacteria grow. During infection, the peptidoglycan can interfere with phagocytosis, is mitogenic (stimulates mitosis of lymphocytes), and has pyrogenic activity (induces fever). The Gram positive cell wall may also include other components such as teichoic and lipoteichoic acids and complex

polysaccharides (usually called C polysaccharides). Proteins such as the M protein of streptococci and R protein of staphylococci also associate with the peptidoglycan.¹¹

Gram Negative Bacteria:

Gram negative cell walls are more complex than Gram positive cell walls, both structurally and chemically. Structurally, a Gram negative cell wall contains two layers external to the cytoplasmic membrane. Immediately external to the cytoplasmic membrane is a thin peptidoglycan layer, which accounts for only 5% to 10% of the Gram negative cell wall by weight. There are no teichoic or lipoteichoic acids in the Gram negative cell wall. External to the peptidoglycan layer is the outer membrane, which is unique to Gram negative bacteria. The area between the external surface of the cytoplasmic membrane and the internal surface of the outer membrane is referred to as the periplasmic space. In the case of pathogenic Gram negative species, many of the lytic virulence factors such as collagenases, hyaluronidases, proteases, and beta-lactamase are in the periplasmic space.¹²

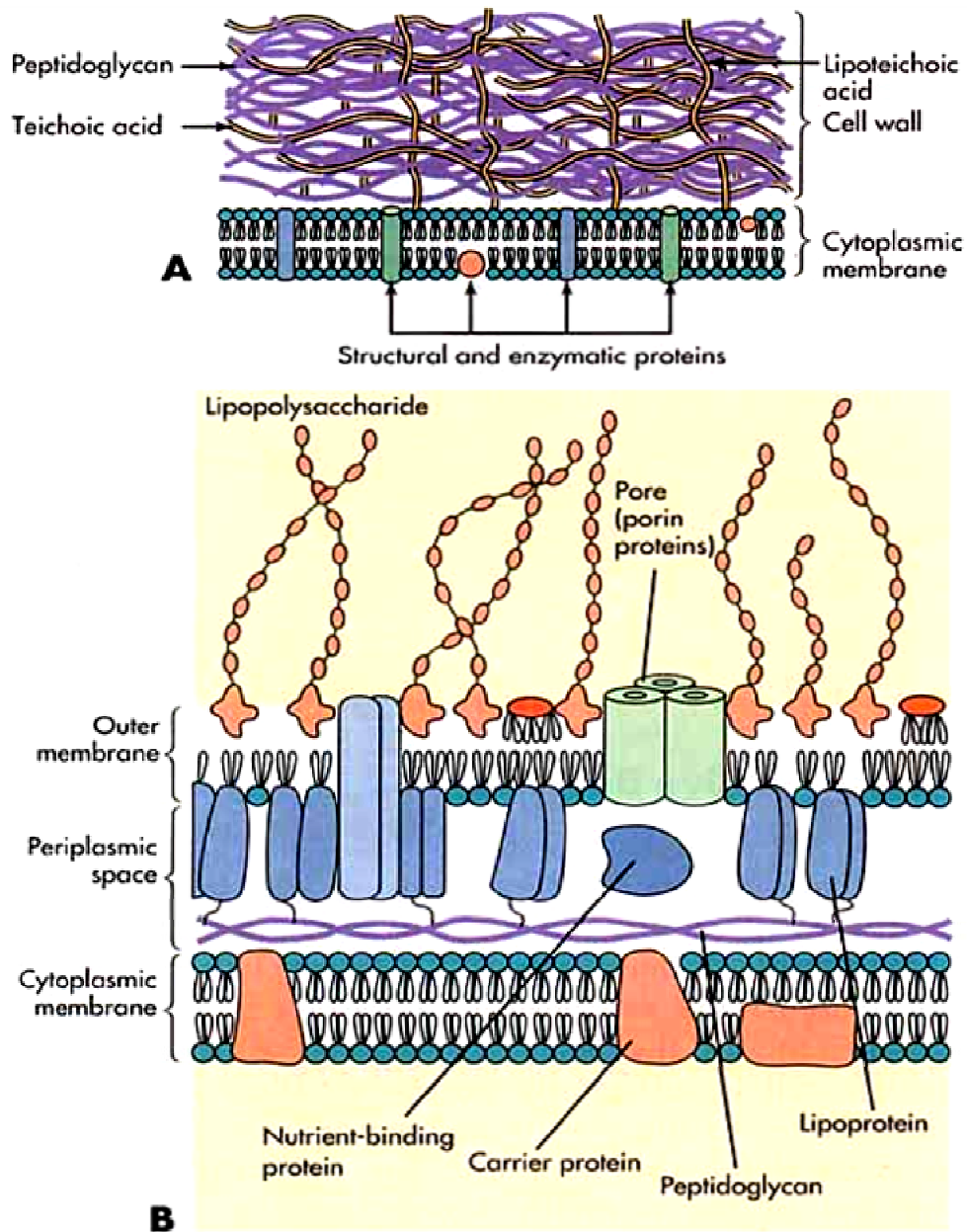


Figure 3: Comparison of the Gram positive and Gram negative bacterial cell walls. (A) Gram positive bacterium has a thick peptidoglycan layer that contains teichoic and lipoteichoic acids. (B) Gram negative bacterium has a thin peptidoglycan layer and an outer membrane that contains lipopolysaccharide, phospholipids, and proteins.¹²

Nanoparticles (NPs) have been used to synthesize or to improve the remedial efficacy of antibacterial agents.¹³⁻¹⁹ This application may benefit from one or a few combinations of the properties of NPs:

- Act as a carrier of drugs to effectively pass through cell membranes.
- Able to concentrate drugs on their surfaces, resulting in polyvalent effects.
- Specifically attack biological targets after modification with target molecules.

NPs for this purpose are generally synthesized by using various metals and polymers.^{20,21} Unfortunately, the undesirable properties such as cellular toxicity and instability of these NPs limit their application.^{22,23} On the other hand, gold nanoparticles (GNPs) have attracted a significant interest because of convenient surface bioconjugation, remarkable plasmon-resonant optical properties, chemical stability and non-toxicity.²⁴⁻²⁷ Studies have also shown that the GNPs are useful to improve the efficacy, drug delivery, target specificity and biodistribution of the drugs which enhances the antibacterial activity against MDR.²⁰⁻²⁷ For the synthesis of GNPs, various wet chemical methods employing various polar and nonpolar solvents have been used.^{28,29} Among them, the most common methods includes the reduction of tetrachloroauric acid (HAuCl_4) by excess sodium borohydride (NaBH_4) or sodium citrate in the presence of stabilizing/ capping ligands such as citrate, thiolates, amines, phosphanes, carbonyls, dendrimers, hydroquinones and surfactants. For example, the use of hydroquinone, a suspected carcinogen, with traditional citrates methods leaves the product GNPs with trace amounts of organic solvents. This raises environmental concerns and also limits the biocompatibility and biomedical application of GNPs, because of its cellular toxicity.

However, the use of complicated non-bio/ non-ecofriendly chemical synthesis processes and dependence on external sources (such as laser pulses) for the synthesis and/or the activation of GNPs, limits their environmental/bio-compatibility.³⁰⁻³⁴ Studies have demonstrated that the size of the GNPs strongly influence their physical, chemical and biological properties.^{35,36} Therefore, there is a need for environmentally friendly synthesis of GNPs with different sizes for various biomedical applications including those with antibacterial activity.³⁷

This report is focused on the antibacterial activity of dGNPs which were synthesized by employing a ‘completely green’ method as shown in our previously published article.³⁸ dGNPs of three different sizes were synthesized having average diameter of 25 nm, 60 nm, and 120 nm (± 5). Resulting dGNPs were nearly spherical, monodispersed, stable, and water soluble. The dGNPs were prepared using dextrose as both reducing and capping agent.

We have explored the antibacterial activity of the sugar encapsulated biocompatible GNPs against both Gram-negative (*Escherichia coli*) and Gram-positive (*Staphylococcus epidermidis*) bacteria. Investigation of the bacterial growth kinetics and growth inhibition in the presence of the dGNPs at various concentrations was performed using a real-time spectrophotometric assay. Antibacterial activity and efficacy were further validated by turbidimetry and spread plate assays. To understand the mechanism of action, we performed fluorescence microscopy and observed ultrathin slices of dGNP treated bacterial cells under the transmission electron microscope (TEM).

MATERIALS AND METHODS

Reagents and Material:

KAuCl₄/ HAuCl₄, Luria-Bertani (LB) broth, LB agar, Soy tryptic agar, propidium iodide and dextrose were purchased from Aldrich, St. Louis, MO. *E. coli* and *S. epidermidies* were purchased from Invitrogen, Carlsbad, CA or obtained from Western Kentucky University culture collection. Analytical grade chemicals were typically used.

Synthesis and Characterization of dGNPs:

Gold nanoparticles were synthesized according to our previously published, environmentally benign, biofriendly, single-step/single-phase synthesis method.³⁸ In this method dextrose was used as a reducing agent as well as a capping agent for the reduction of Au³⁺ ions in an aqueous buffer at room temperature and atmospheric pressure. The synthesized dGNPs were characterized using different analytical techniques. To determine the morphology of dGNPs, the absorption spectra were observed using Perkin Elmer Lambda 35 UV/vis spectrophotometer. The shape and size of the dGNPs were further confirmed by JEOL TEM. EDS (Energy Dispersive Spectroscopy) was performed to analyze the elemental composition of nanoparticles using JEOL JSM -5400 LV with IXRF system.

Quantification of dGNPs:

We determine the concentration of dGNP using reported methods for calculating gold atoms per GNP.^{10,39,40} One mole of any substance contains 6.023×10^{23} atoms (Avogadro's number). For the synthesis of 120 nm GNP, 0.5 mM concentration of Au³⁺ was used. The total number of Au atoms in the solution = 0.500×10^{-3} mol/ liter $\times 6.023 \times 10^{23}$ atoms/ mol = 3.012×10^{20} atoms/ liter.³⁸ We have used the reported equation, for

calculating number of gold atoms, $N_{Au} = (dGNP/nm)^3 \times 31$, where dGNP is the diameter of spherical dGNP. ¹⁰ Typical dGNP of 120 nm size will have, $(120nm/nm)^3 \times 31 = 5.3568 \times 10^7 N_{Au}$. Therefore total number of nanoparticles (in 1 mL)/ $= N_{Au}$ (in 1 mL sample)/ N_{Au} (in one GNP). Concentration of dGNP with average diameter of 120 nm, in one mL sample = 3.115×10^{17} atoms/ 5.3568×10^7 atoms = 5.622×10^9 GNPs/mL. Different sizes/ concentrations of dGNPs were obtained by synthesizing them in different volumes following the above method. All values for calculation of number of dGNPs are within the error range of 10^2 NPs/ mL.

Determination of Antibacterial Activity of Sugar Encapsulated GNPs:

For each antibacterial experiment the bacteria were cultured fresh by inoculating 100 μ L of bacterial glycerol stock into 10 mL of sterile LB or minimal liquid medium in a culture tube. The bacteria were allowed to grow overnight in an incubator maintained at 37 °C and shaken at 150 rpm. For all the experiments dGNPs were washed several times with sterile water and then resuspended in the nanopure water

Turbidimetry:

Turbidimetry is a microbiological assay performed for measuring MIC (minimum inhibitory concentration) of dGNPs against *E. coli*. Various concentrations of dGNPs with average diameter of 120 nm (2×10^{10} , 4×10^{10} , 8×10^{10} , 16×10^{10} NPs/mL), 60 nm (2×10^{11} , 4×10^{11} , 8×10^{11} , 16×10^{11} NPs/mL), 25 nm (16×10^{12} , 32×10^{12} , 64×10^{12} , 128×10^{12} NPs/mL) were inoculated with 10^9 CFU/cm³ in a series of culture tubes containing 4 mL of sterile liquid media. Control experiments were performed by inoculating the media with *E. coli* in the absence of dGNPs. All the tubes were incubated at 37 °C and

optical density at 600 nm was monitored for 12 h. Increase in OD indicates the proliferation/growth of bacteria.^{41,42}

Spread Plate Technique:

The bacteria were grown in a series of culture tubes containing 4 mL of sterile liquid media with various concentrations of dGNPs. Cultures from selected concentrations and growth points (12 h) were spread onto Luria Bertani or Soy tryptic agar plates and incubated at 37 °C for 12 h to estimate the number of viable bacteria.⁴³

Agar Plate Diffusion:

The potency of the antibacterial agent was studied by agar plate diffusion method; where in the suspension of the bacteria containing 10^9 CFU/mL was added to sterile nutrient agar medium at 37 °C and the mixture was allowed to solidify in a petri dish.⁴⁴⁻⁴⁵ Wells of diameter 0.630 cm were punched in agar plate and filled with 50 μ L of either various concentrations of nanoparticle suspension (sample) or kanamycin (standard) or sterile water (control). Nanoparticles were allowed to diffuse into the agar for one hour at 4 °C and the plates were then incubated for 12 h at 37 °C. After incubation, the radius of the zone of bacterial-growth inhibition was measured with an accuracy of ± 0.1 mm. The mean inhibition-zone radius was determined. All the experiments were repeated thrice.

Fluorescence Assay:

The bacteria were cultured in liquid media in the presence of dGNPs with different concentrations for 12 h at 37 °C. The samples were collected and centrifuged at 6000 rpm for 3 min and washed twice with Phosphate Buffer Saline (PBS) (pH ~ 7.2). These bacterial cells were incubated with propidium iodide (3 μ M in PBS) in the dark for 30 min at room temperature. Fluorescence detection was performed on 10 μ L of the

bacterial suspension that was placed on a glass slide and observed under scanning Leica fluorescence microscope.¹⁰ Positive control was prepared by treating the bacterial suspension with 100 % ethyl alcohol for 15 min.

Preparation for Cross-Section of the Bacterial Cells:

Ultrastructural changes induced by dGNP treatment were studied under an electron microscope. Cultures of the two bacterial strains were fixed by mixing with equal volumes of a 2x fixative solution to give final concentrations of 2.0 % w/v paraformaldehyde and 2.5 % w/v glutaraldehyde in 50 mM sodium cacodylate buffer (pH 7.4). After incubating with fixative for 2 h at room temperature, the fixed samples were washed and centrifuged twice; the supernatant was discarded, and the pellet was resuspended in 50 mM sodium cacodylate buffer. The same process was followed during all subsequent solution changes. Samples were post fixed for 1 h at 25 °C with 1% w/v osmium tetroxide in 50 mM sodium cacodylate buffer. The post fixed samples were washed with nanopure water twice, and then dehydrated in a graded ethanol series (once in 25%, 50%, 75%, and 95% and thrice in 100 % ethanol for 10 min each). The dehydrated samples were infiltrated with Spurr's epoxy resin (once in 33%, 66%, 95% and thrice in 100% resin for 1 h each) and then left overnight in 100% resin. The samples were centrifuged through fresh resin in BEEM capsules and hardened at 70 °C for 18 h. Ultra-thin sections of the pelleted samples were cut on an RMC MT-X ultra microtome using glass knives. Sections were stained with 2 % aqueous uranyl acetate and Reynold's lead citrate for 15 min and 3 min respectively, and examined using a JEOL-100CX transmission electron microscope.^{46,47}

RESULTS AND DISCUSSIONS

The use of non-bio/ non-ecofriendly synthesis processes, cellular toxicity and instability of these nanoparticles limits their application. Taking these into consideration, we explored the antibacterial properties of stable, biocompatible eco-friendly dGNPs.

Synthesis and Characterization of dGNPs:

Three different sizes of dGNPs [25 nm, 60 nm and 120 nm (± 5 nm)] were synthesized using the previously published method in which dextrose was used as a capping and reducing agent (Figure 5).³⁸ dGNPs of different sizes were produced by varying the concentrations of KAuCl₄. The properties of the synthesized dGNPs were characterized using TEM, UV/vis, FTIR and EDS.

The presence of the dextrose on the surface of dGNPs was determined by the Benedict's test. dGNPs were able to reduce copper sulphate solution which was observed by a color change from blue to brick red color (Figure 6).⁴⁸ Further, the presence of unreduced hydroxyl groups on the dGNPs was determined by the volumetric acid-base titration. In this experiment, the dGNPs were added to the mixture of pyridine and acetic anhydride (2:1).

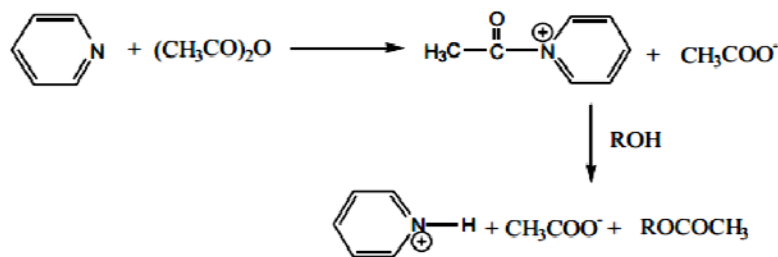


Figure 4: Reaction scheme showing the acetylation mechanism of alcohols with Ac₂O in pyridine.

This reaction was kept for 30 hrs at 60°C for complete acetylation of hydroxyl groups. The resultant mixture was added to 200 ml ice cold water and titrated against 0.5 M NaOH with phenolphthalein indicator until the mixture turns pink (Figure 7). Thus the results confirmed the presence of reducing hydroxyl groups on the surface of dGNPs.⁴⁹

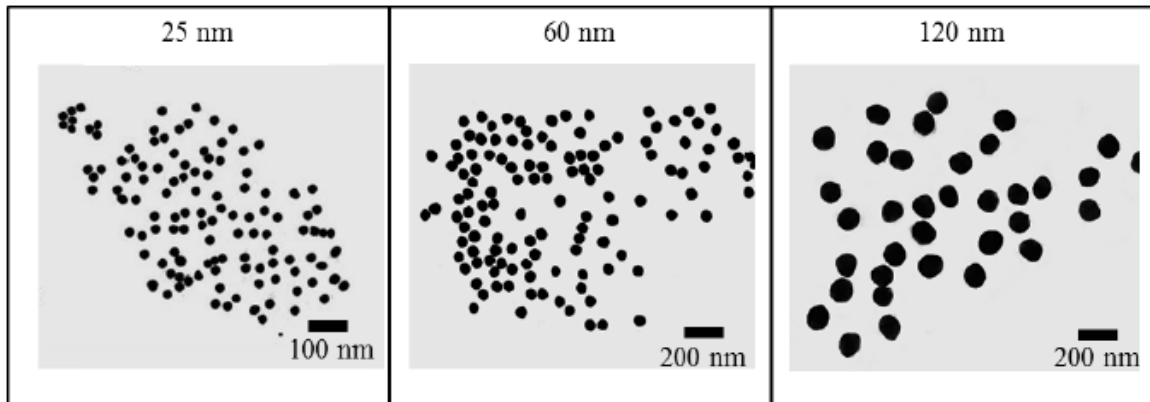


Figure 5: Representative TEM images of dGNPs of three sizes 25 ± 5 nm (scale bar = 100 nm); 60 ± 5 nm (scale bar = 200 nm); 120 nm (scale bar = 200 nm)

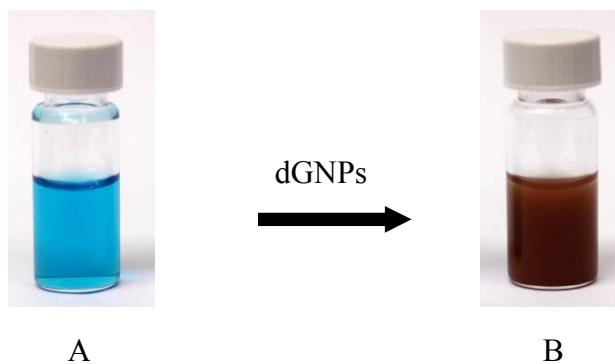


Figure 6: Shows the digital images of (A) unreduced benedicts reagent and (B) reduced benedicts reagent in the presence of dGNPs

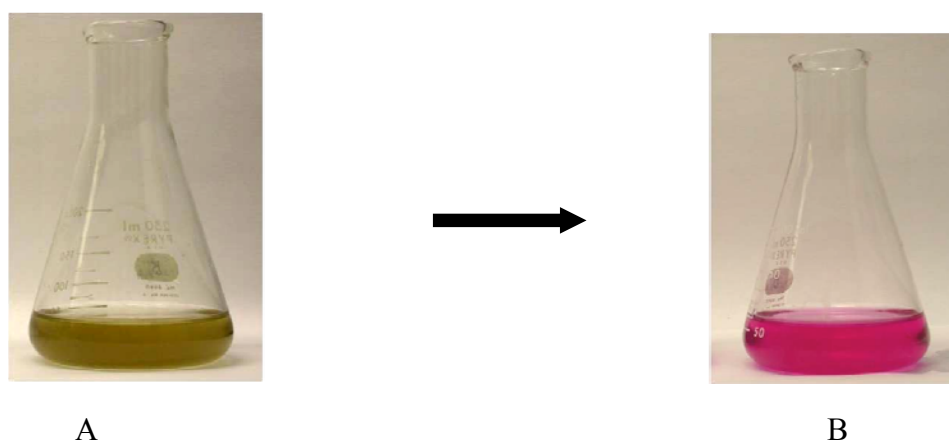


Figure 7: Shows the digital images of conical flask before (A) and after (B) acid-base titration indicating the end point at which the total acid (reaction mixture) in the reaction is neutralized using a base (NaOH)

Antibacterial Activity:

To determine the antibacterial activity of dGNPs, we performed both liquid broth and solid agar plate based growth studies on *E. coli*. The dGNPs of different sizes were tested for their antibacterial activity at various concentrations against *E. coli*. Before performing the actual antibacterial experiment the GNPs were tested for their stability by suspending the nanoparticles in sterile liquid media in culture tube and kept in an incubator shaker at 37°C. The dGNPs were found to be intact/ stable (no cluster/precipitation) for more than 48 hrs. In the tube assay, the bacterial cells were grown in the presence of dGNPs and the growth was monitored hourly by measuring the optical density (OD) at 600 nm for 12 h. Blank samples were prepared by suspending the dGNPs in sterile liquid medium and processed in the same condition as that of samples. Any absorption due to dGNPs was autocorrected using a blank sample. Results were plotted with the OD on Y-axis against the time on X-axis (Figure 8). Both the 120 nm and 60 nm dGNPs were found to inhibit the proliferation of *E. coli*, in a concentration dependent manner with minimum inhibitory concentrations (MIC) at 16×10^{10} NPs/mL and 16×10^{11} NPs/mL respectively. The 25 nm dGNPs did not significantly affect the proliferation of *E. coli* even at a concentration as high as 128×10^{12} NP/mL. The 120 nm dGNPs were found to be the most potent antibacterial agent compared with the 60 nm which in turn were more potent than the 25 nm (Figure 8). The growth kinetic data clearly suggested that the antibacterial activity was directly proportional to the increase in size of dGNPs.

The antibacterial activity exhibited by dGNPs could be attributed to the presence of free Au^{3+} ions that remained in solution when the dGNPs were suspended in water or

due to changes in pH, since the bacterial activity is sensitive to both of these factors. To quantify the free Au^{3+} ions in the suspension, the dGNPs precipitated by centrifugation and the supernatant was tested for the presence of free Au^{3+} ions by measuring the absorbance at 290 nm. The near zero absorbance at 290 nm, showed the absence of any free Au^{3+} ion (data not shown) suggesting that the free Au^{3+} ion concentration in the dGNPs suspension was insignificant and, therefore, not responsible for antibacterial activity. In addition, the pH of the dGNPs suspensions was at 7.2-7.4 which is the normal pH range for the microorganisms environment. Hence, pH could not have been responsible for the antibacterial activity. Taken together, the results suggested that the antibacterial activity was due to the dGNPs and not due to free Au^{3+} ion or change in pH.

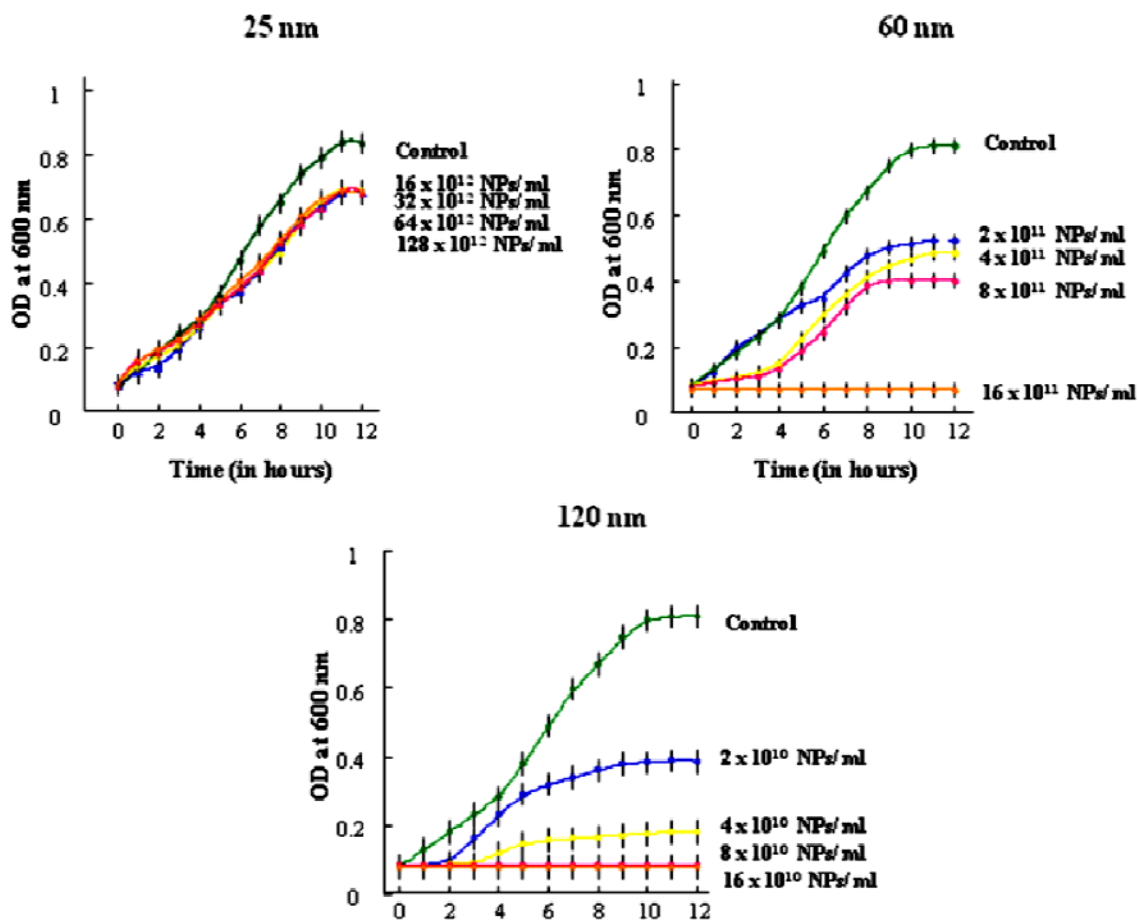


Figure 8: Effect of different sizes of dextrose encapsulated GNPs on the growth of *E. coli*. Growth analysis curves were measured by monitoring the optical density (OD) at 600 nm and the *E. coli* was treated with dGNPs of sizes: 25 ± 5 nm; 60 ± 5 nm and 120 ± 5 nm at different concentrations (NPs/ ml).

Results of the growth assay indicated that the presence of dGNPs inhibited the growth of *E. coli*, representing the bacteriostatic property of the dGNPs. In order to confirm whether dGNPs exhibited bactericidal action, spread plate technique was used. The cultures in the liquid broth that were treated with different sizes of dGNPs for 12 h [the time required by control to reach the stationary phase (complete growth)] were plated on fresh LB agar media. The results given in (Figure 9-I-A & B) indicated that the number of colonies on the agar plate significantly decreased with increase in the size of dGNPs. The antibacterial potency of dGNPs increased as the size increased (25 nm < 60 nm < 120 nm). Furthermore, the growth of the colonies on the agar plate demonstrated that within one size of dGNPs, the bactericidal effect was concentration dependent (Figure 9-I-A & B). The above results from the agar spread plate methods confirmed that the dGNPs exhibited bactericidal properties. Also, when compared with the potency of standard antibiotic Kanamycin (Figure 9-II-A & B), the dGNPs with sizes 120 nm and 60 nm, at their respective highest concentration (16×10^{10} NPs/mL and 16×10^{11} NPs/mL respectively), retarded the bacterial growth to the same extent as 5.0 mg/mL concentration of kanamycin (Figure 9-III-A).

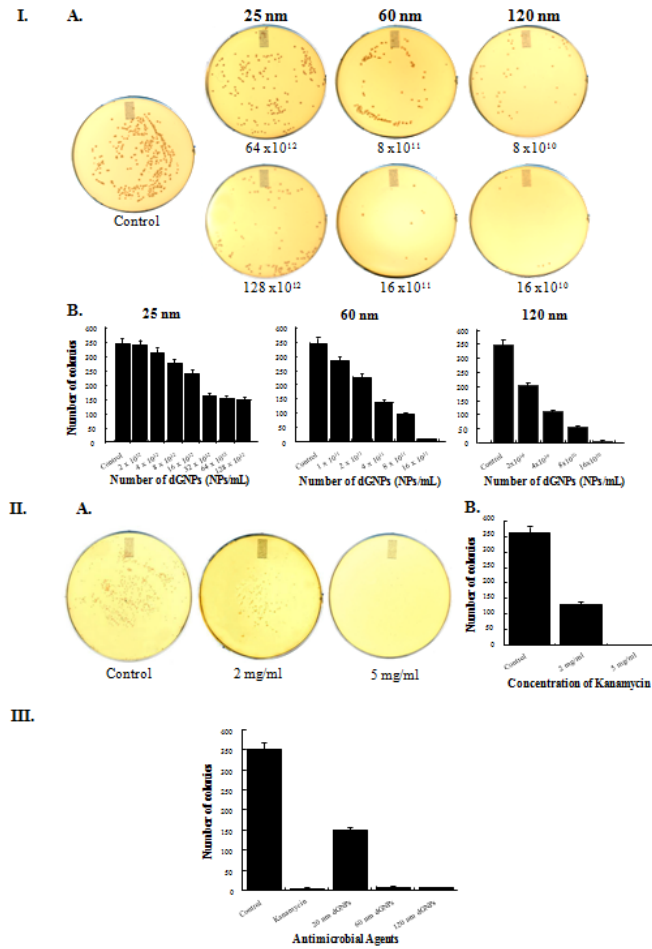


Figure 9: I.(A) Plate assay showing the number of viable cells recovered after the treatment of *E. coli* without (control) or with presence of dGNPs of sizes; 25 ± 5 nm, 60 ± 5 nm, and 120 ± 5 nm at different concentrations (NPs/ ml). I.(B) Graphs plotted for number of *E.coli* colonies recovered, against concentration of dGNPs. II.(A) Plate assay showing the number of viable cells recovered after the treatment of *E. coli* without (control) or with different concentrations of kanamycin. II.(B) Graphs plotted for number of *E.coli* colonies recovered against different kanamycin concentrations. III. Comparison plot for the number of *E.coli* colonies recovered against different antimicrobial agents (dGNPs & kanamycin).

Agar plate diffusion is a microbiological assay used for comparing the potency of unknown antimicrobial with a known standard antibiotic against the bacteria grown in solid media. In this context, to determine the antibacterial potency of the GNPs, we performed agar plate diffusion (APD) assay. We performed the APD assay using dGNPs (Figure 10-I-A & B) and a standard antibiotic kanamycin, (Figure 10-II-A & B) against *E. coli*. The results indicated that the 120 nm and 60 nm GNPs attenuated the bacterial growth with increasing number of nanoparticles [NPs/mL (Table. 1)]. However, the 25 nm GNPs did not show any zone of inhibition, indicating that this size was an inefficient antibacterial agent. At $1/10^{\text{th}}$ the number of NPs of 120 nm showed the same extent of radius of inhibition zone as that shown by number of NPs of 60 nm, which proves 120 nm to be more efficient antibacterial agent.

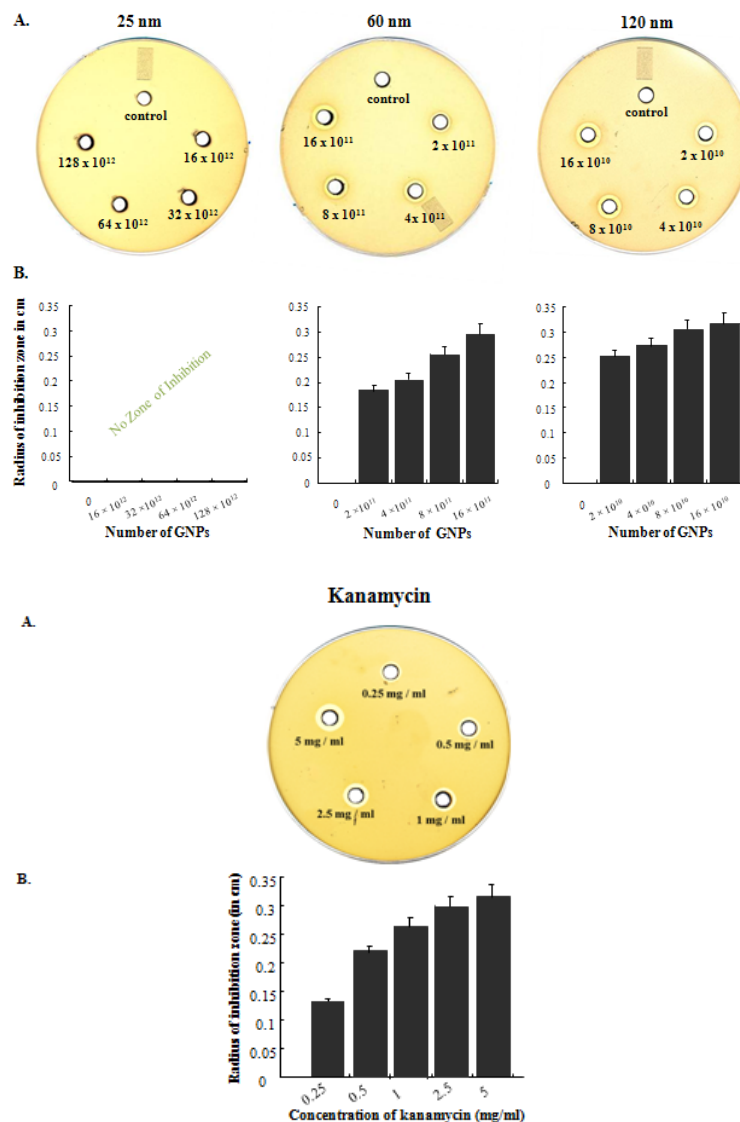


Figure 10: I. Potency of the GNPs as anti-bacterial agents against *E. coli* shown as (A) Images of petri dishes showing the retardation of bacterial growth at different concentrations of GNPs of sizes 25±5 nm, 60±5 nm, and 120±5 nm. (B) Graphs plotted with averaged radius of inhibition zone against the concentrations of the GNPs. II. (A) Potency of the kanamycin against *E. coli*. Image of petri dishes showing the retardation of bacterial growth at different concentrations of kanamycin. (B) Graphs plotted with averaged radius of inhibition zone against the concentrations of kanamycin.

Type of Bacteria	120 nm	60 nm	25 nm
<i>E. coli</i>	16 x 10 ¹⁰ NPs/ ml (± 10 ² NPs/ ml)	16 x 10 ¹¹ NPs/ ml (± 10 ² NPs/ ml)	128 x 10 ¹² NPs/ ml (± 10 ² NPs/ ml)
<i>S. epidermidis</i>	16 x 10 ¹⁰ NPs/ ml (± 10 ² NPs/ ml)	16 x 10 ¹¹ NPs/ ml (± 10 ² NPs/ ml)	128 x 10 ¹² NPs/ ml (± 10 ² NPs/ ml)

Table 1: Representing concentrations of dGNPs of three different sizes used to treat bacteria.

dGNPs Induced Disruption of Bacterial Cells:

To determine the mechanism of the antibacterial activity of dGNPs, time dependent action of dGNPs on the morphology of bacterial cell was monitored. This was done by collecting *E. coli* cells treated with dGNPs at different time points and were processed for cross sectional analysis. TEM analysis of the cross sections of untreated cells showed that the membrane integrity remained intact at different time points even after the stationary phase (after 12 hours) (Figure 11-I-a & b). However, bacteria treated with 120 nm and 60 nm dGNPs showed gradual morphological changes within six hours. Initially, the dGNPs were observed to anchor onto the surface of the cell at several sites (Figure 11-II-a). Gradually, the sites where dGNPs lodged, showed the formation of perforations or Outer Membrane Vesicles (OMVs) on the membrane, which eventually resulted into complete cell lysis (Figure 11-II-b & c).^{50,51}

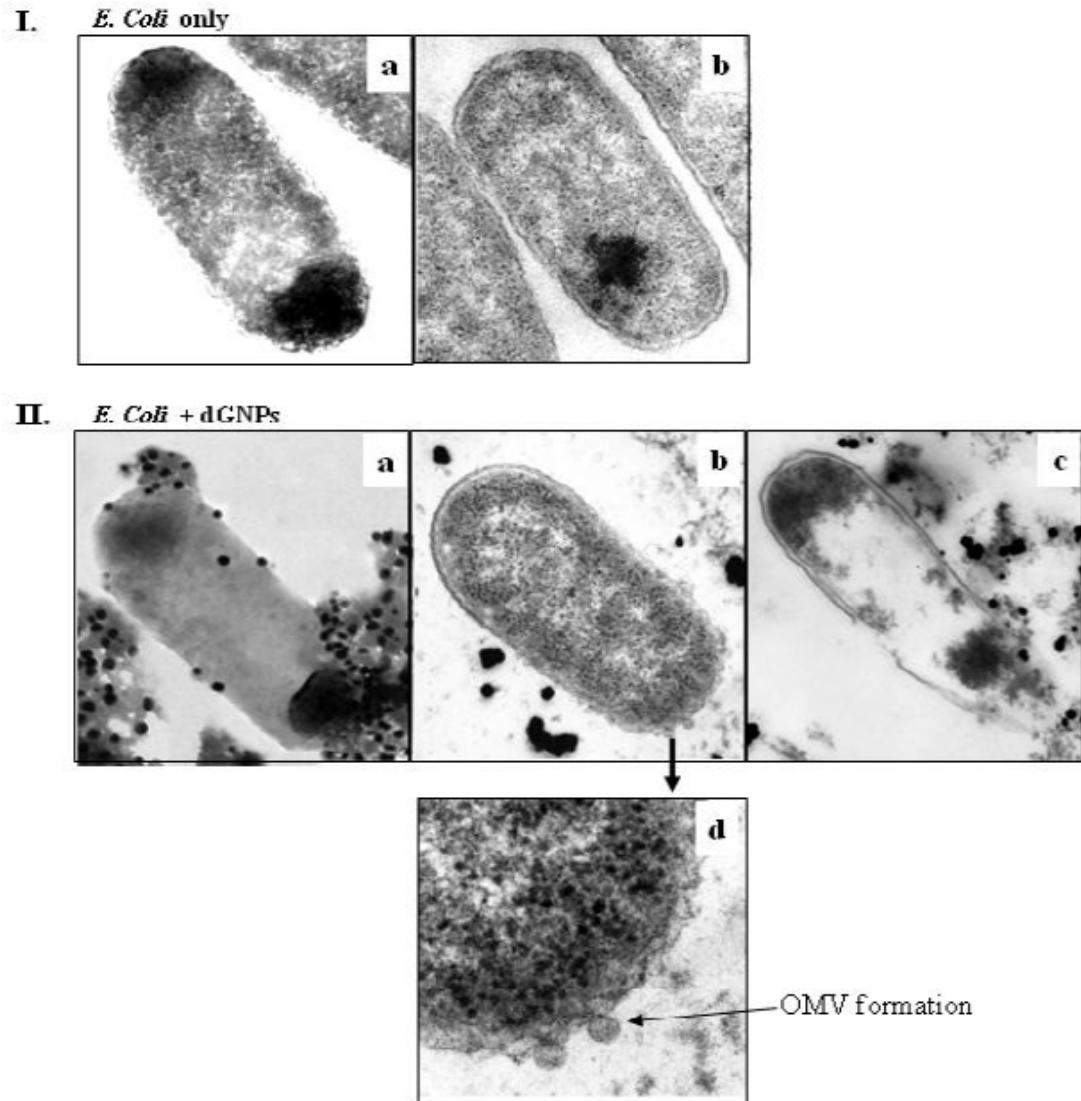


Figure 11: Visualization of dGNP induced morphological changes in *E. coli* cell membranes under the TEM. I-a. Morphology of the untreated *E. coli* cell at 0 h; I-b. Cross-section of the untreated *E. coli* cell after 12 h; II-a. Interaction of dGNPs with *E. coli* cell at 0 h; II-b. Cross-section of the dGNPs treated *E. coli* cell after 6 h showing the initiation of the cell disruption by the formation of outer membrane vesicles (OMVs); II-c. Cross-section of the lysed *E. coli* cell after 12 h of treatment with dGNPs; II-d. The magnified view of OMV formation, which represents the initiation of disruption of cell membrane.

To investigate the effect of various sizes of dGNPs on the cell permeability, cells were treated with propidium iodide (PI). PI is a fluorescent dye, which specifically binds with nucleic acid and produce enhanced fluorescence. However, PI cannot cross intact membranes and is excluded from viable cells.¹⁰ Thus, in the presence of PI, cells with permeable membrane (lysed or damaged cell membrane) will fluoresce under the fluorescence microscope. For this study, we incubated fresh *E. coli* cultures with different sizes of dGNPs and then treated with PI to assess the integrity of the cell membrane. Fluorescence images showed that the permeability of dGNP treated bacteria was 92% for 120 nm, 87% for 60 nm and very minimal permeability of less than 13 % for 25 nm (Figure 12-A). The permeability of the cell membrane increased significantly with exposure to increase in the size of dGNPs and also with the increase in the concentration of dGNPs as evidenced clearly in Figure 12-B. Therefore, exposure of the cells to dGNPs leads to the disruption of the integrity of the cell membrane causing increased permeability and possible leaching of the cell materials. These results indicated the size dependent effect of the dGNPs on bacterial membrane through the time dependent leaching /disruption. It must be noted that the mechanism of interaction between the cell membrane and the dGNPs needs to be investigated.

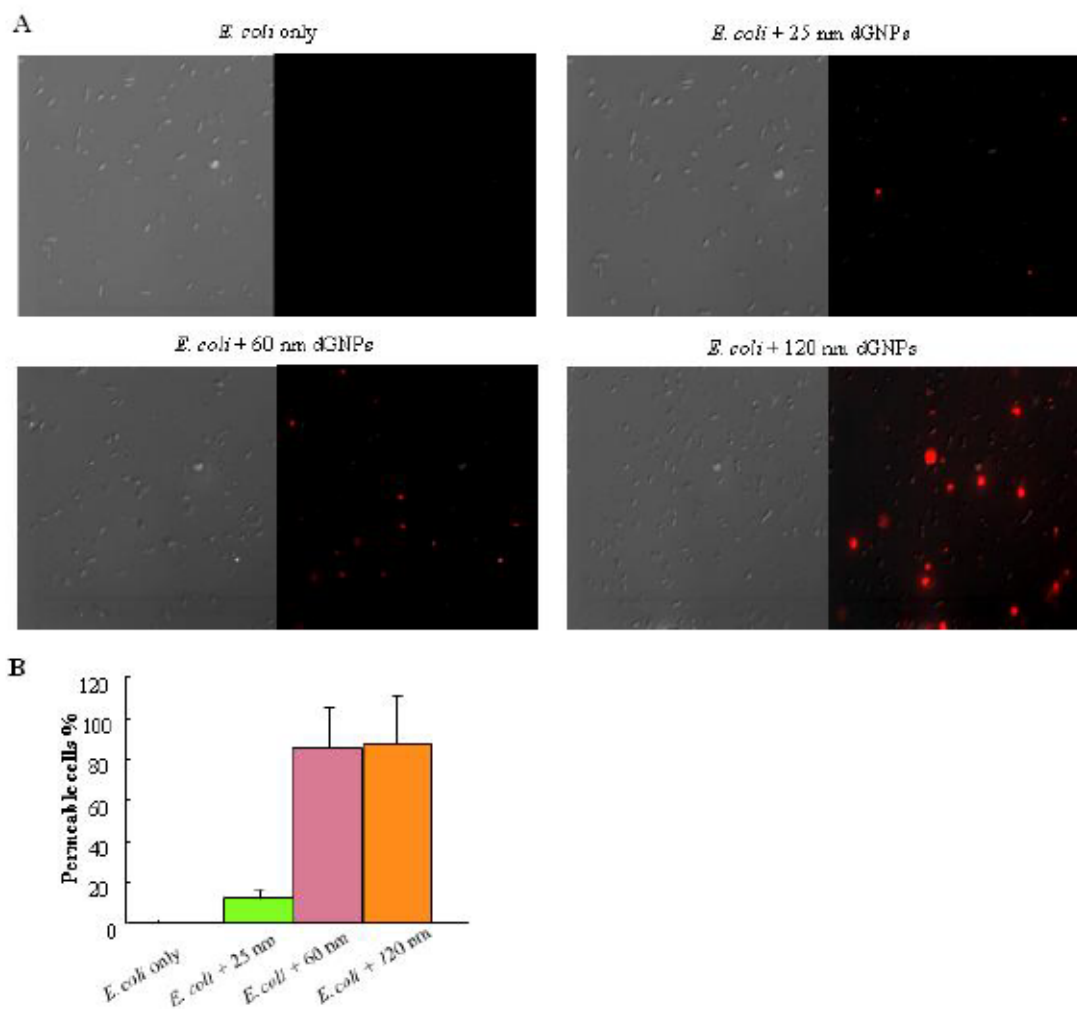


Figure 12: Monitoring dGNPs induced permeability of *E. coli* cell membranes and leakage of nucleic acids via propidium iodide. (A) The left half shows an image in the differential interference contrast mode while the right half shows the corresponding fluorescence image. (B) The percentage of cells with permeable membranes from 5 or more fields of view obtained by two independent experiments.

To determine the antibacterial nature of dGNPs, we further performed antibacterial experiments against *Staphylococcus epidermidis*. *Staphylococcus* is a genus of Gram positive bacteria, which resides normally on the skin and mucous membranes of human and other organisms causing a wide array of disease.⁵²⁻⁵⁴ Plate based growth studies showed similar results to those against *E. coli*, indicating less number of recovered cells with increasing size of dGNPs as well as with increase in the concentration of particles. Also potency of dGNPs (Figure 13- I-A & B) with sizes 120 nm and 60 nm at their respective highest concentration (16×10^{10} NPs/mL and 16×10^{11} NPs/mL respectively), was found to be similar to that of standard antibiotic kanamycin (Figure 13-II-A & B), at concentration of 2.5 mg/mL (Figure 13-III).

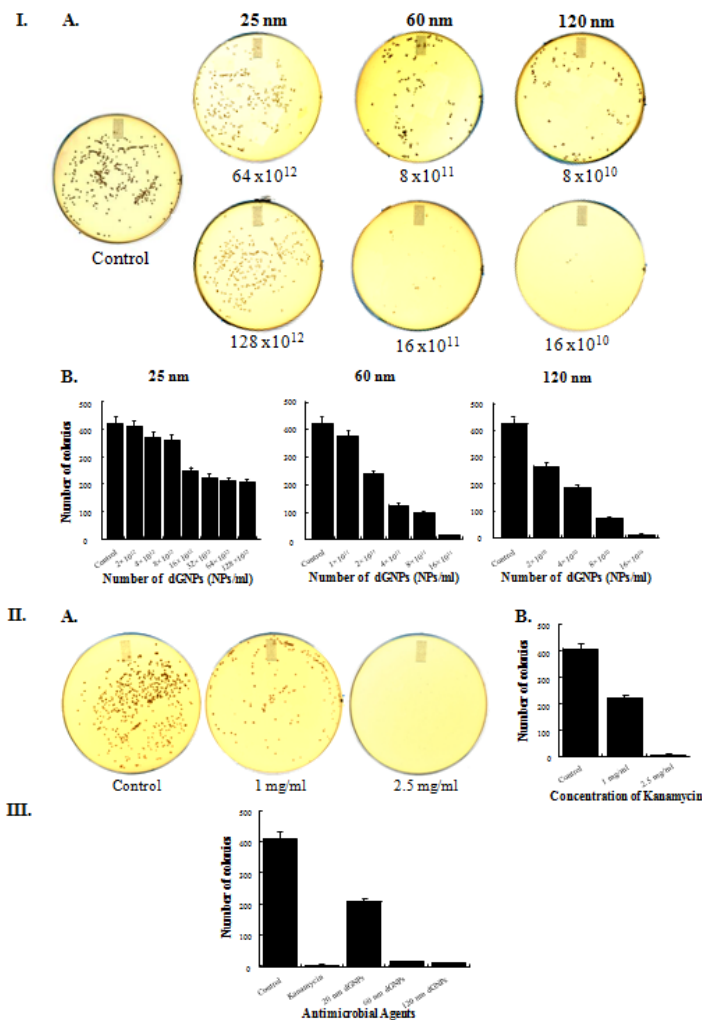


Figure 13: I.(A) Plate assay showing the number of viable cells recovered after the treatment of *S. epidermidis* without (control) or with presence of GNPs of sizes; 25 ± 5 nm, 60 ± 5 nm, and 120 ± 5 nm at different concentrations (NPs/ ml). I.(B) Graphs plotted for number of *S. epidermidis* colonies recovered, against concentration of dGNPs. II.(A) Plate assay showing the number of viable cells recovered after the treatment of *S. epidermidis* without (control) or with presence of different concentrations of kanamycin. II.(B) Graphs plotted for number of *S. epidermidis* colonies recovered against different kanamycin concentrations. III. Comparison plot of the number of *S. epidermidis* colonies recovered on against different microbial agents (dGNPs & kanamycin).

Results of the TEM and fluorescence microscopy analysis suggested that the antibacterial activity of dGNPs against *S. epidermidis* also occurred through the disruption of bacterial cellular membrane, which was similar to that of *E. coli* (Figure 14 & 15).

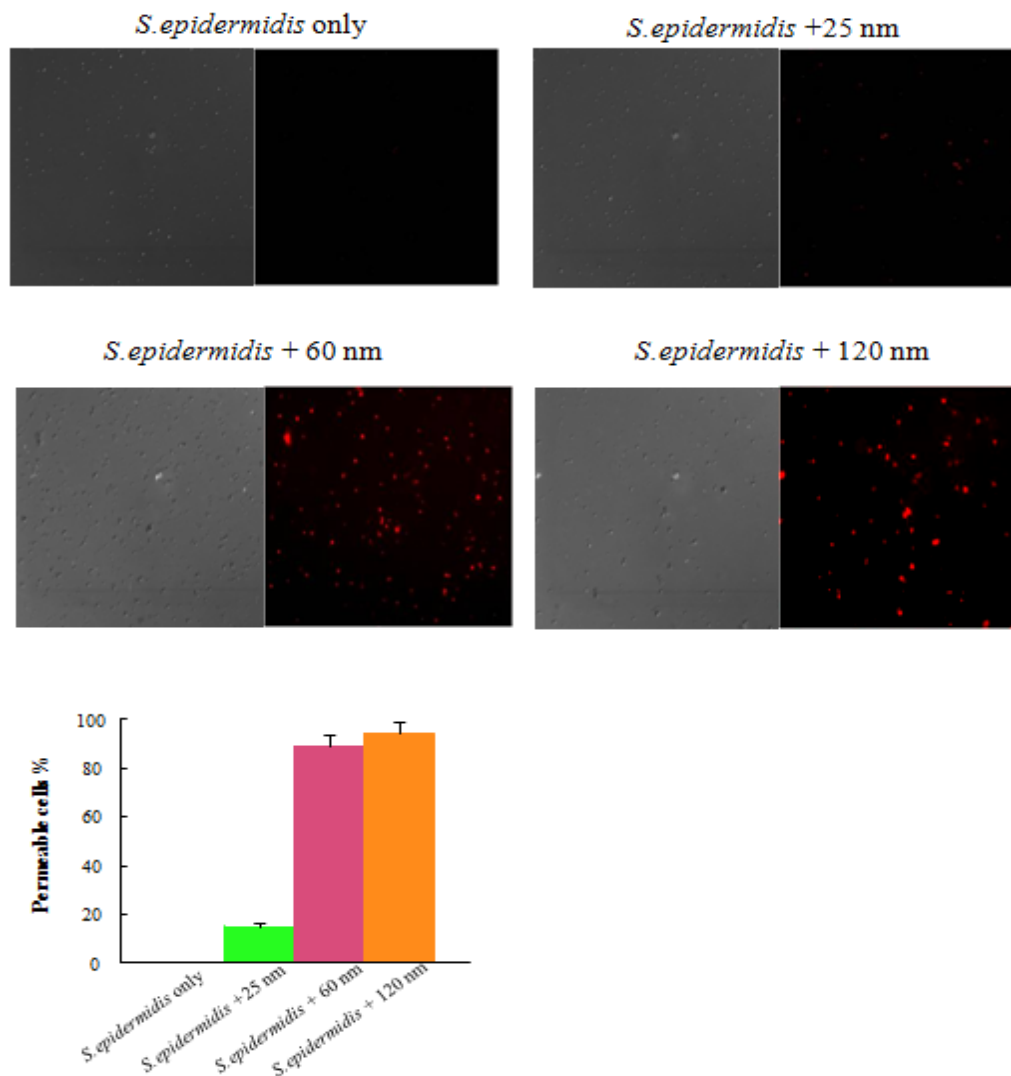
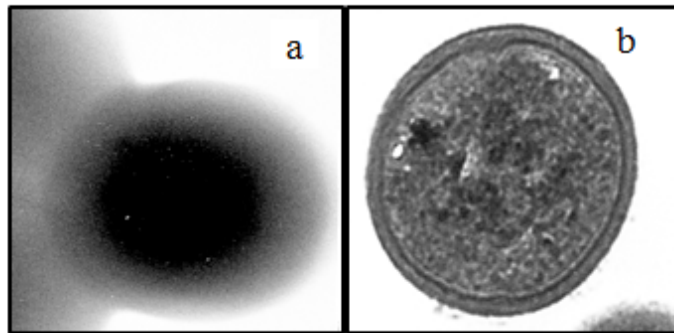


Figure 14: Monitoring dGNPs induced permeability of *S. epidermidis* cell membranes and leakage of nucleic acids via propidium iodide. (A) The left half shows an image in the differential interference contrast mode while the right half shows the corresponding fluorescence image. (B) The percentage of cells with permeable membranes from 5 or more fields of view obtained by two independent experiments.

I. *S.epidermidis* only



II. *S.epidermidis* + GNPs

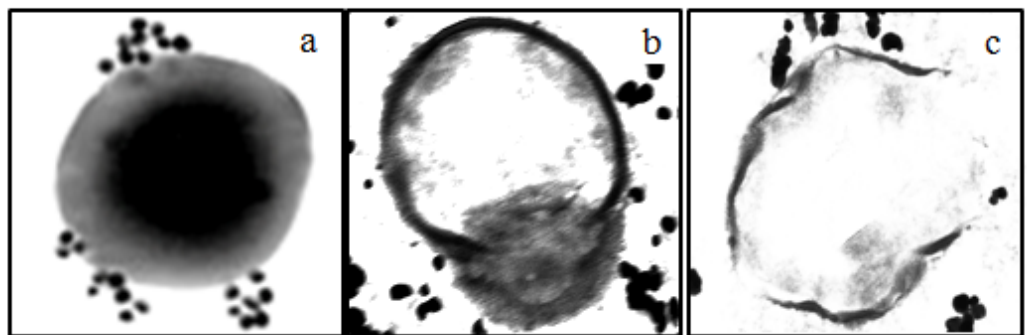


Figure 15: Visualization of dGNP induced morphological changes in *S. epidermidis* cell membranes under the TEM. I-a. Morphology of the untreated *S. epidermidis* cell at 0 h; I-b. Cross-section of the untreated *S. epidermidis* cell after 12 h; II-a. Interaction of dGNPs with *S. epidermidis* cell at 0 h; II-b. Cross-section of the dGNPs treated *S. epidermidis* cell after 6 h showing the initiation of the cell disruption; II-c. Cross-section of the lysed *S. epidermidis* cell after 12 h of treatment with dGNPs.

Overall the result suggested similar potency and membrane disruption process/mechanism for the antibacterial activity of dGNPs towards Gram negative as well as Gram positive bacteria. Dextrose is a polyhydroxylated molecule, which can act both as a hydrogen bond donor as well as a hydrogen bond acceptor. Though modified, the capping ligand dextrose still possessed the properties of reducing sugar (unmodified dextrose). Benedicts test was performed to confirm the presence of reducing sugar. Also the presence of unmodified (unreduced) hydroxyl group was confirmed using volumetric titration. The presence of reducible hydroxyl group can thus be attributed to the strong electrostatic interaction between dGNPs and both gram negative and gram positive bacteria, which in turn lead to the disruption of cell membrane. Thus, this may explain the versatile antibacterial activity of these dGNPs. It may be inferred that the ligand molecule dextrose plays a crucial role in the antibacterial action but the mechanism of interaction remains to be established.

CONCLUSION

Antibacterial activity of bio-friendly/ eco-friendly dextrose encapsulated GNPs of sizes 25 nm, 60 nm and 120 nm (± 5), were investigated. These GNPs showed significant antibacterial activity against both Gram-negative as well as Gram-positive bacteria without the need for external sources of energy. The efficiency of antibacterial activity was directly proportional to the increase in size as well as the concentration of dGNPs. These dGNPs were found to exert their antibacterial action via disruption of the cell membrane leading to possible leakage of the cytoplasmic contents including nucleic acids. These results suggest, it is plausible that the amphoteric nature of dextrose (the capping ligand) might be responsible for the interaction of dGNPs with both the Gram-positive and Gram-negative bacteria which, in turn, leads to the antibacterial activity. The antibacterial property of the dGNPs holds promise for pharmaceutical and disinfectant applications and other biomedical applications. The molecular level interaction between the cell membrane and the dGNPs that causes membrane rupture remains to be established.

FUTURE STUDIES

The advancement of nanotechnology, which is considered as a most promising technology in the future, needs environmental friendly synthesized nanoparticles. The method used in this paper is completely Green Method; hence, this method can find a variety of applications in various fields. Moreover, because of the biocompatibility, it has wide applications in the field of biomedicine. Nanoparticles can also be used in the treatment of various diseases and also in drug delivery. Though our nanoparticles were proved to be antimicrobial, further effort to be made to determine its cytotoxicity and also to explore the other activities of these dGNPs.

REFERENCES

1. Melanie, A. Jerome, Rose. Jean-Yves, B. Gregory, V. L. Lean-Pierre, J. Mark, R. W. *Nature*. **2009**, *4*, 634-641.
2. Burns, C. Spendel, W. U. Puckett, S. Pacey, G. E. *Talanta*. **2006**, *4*, 873-876.
3. <http://www.azonano.com/article.aspx?ArticleID=2407>
4. Salata, O. V. *J. Nanotechnology*. **2004**, *2*, 1-6.
5. Bruchez, M. Moronne, M. Gin, P. Weiss, S. Alivisatos, A. P. *Science*. **1998**, *281*, 2013-2016.
6. Chan, W. C. W. Nie, S. M. *Science*. **1998**, *281*, 2016-2018.
7. Mahtab, R. Rogers, J. P. Murphy, C. J. *J Am Chem Soc*. **1995**, *117*, 9099-9100.
8. So, A. D. Gupta, N. Brahmachari, S. K. Chopra, I. Munos, B. Nathan, C. Outtersson, K. Paccaud, J. P. Payne, D.J. Peeling, R.W. Spigelman, M. Weigelt, J. *Drug Resist Update*. **2011**, *14*, 89-94.
9. Salerno, F. Cazzaniga, M. *Intern Emerg Med*. **2010**, *5*, 45-51.
10. Zhao, Y. Tian, Y. Cui, Y. Liu, W. Ma, W. Jiang, J. *J Am Chem Soc*. **2010**, *132*, 12349–12356.
11. Gregersen, T. *Appl Microbiol Biotechnol*. **1978**, *5*, 123-127.
12. Lugtenberg, S. Van-Alphen, L. *Biochem Biophys Acta*. **1983**, *737*, 51-115.
13. Balland, O. Pinto-Alphandary, H. Viron, A. Puvion, E. Andreumont, A. Couvreur, P. *J Antimicrob Chemother*. **1996**, *37*, 105–115.
14. Rosemary, M. J. MacLaren, I. Pradeep, T. *Langmuir*. **2006**, *22*, 10125–10129.
15. Rosi, N. L. Giljohann, D. A. Thaxton, C. S. Lytton-Jean, A. K. Han, M. S. Mirkin, C. A. *Science*. **2006**, *312*, 1027–1030.

16. Thomas, M. Klibanov, A. M. *Proc Natl Acad Sci U.S.A.* **2003**, *100*, 9138–9143.
17. Cho, E. C. Au, L. Zhang, Q. Xia, Y. *Small*. **2010**, *6*, 517–522.
18. Bowman, M. C. Ballard, T. E. Ackerson, C. J. Feldheim, D. L. Margolis, D. M. Melander, C. *J Am Chem Soc.* **2008**, *130*, 6896–6897.
19. Gu, H. Ho, P. L. Tong, E. Wang, L. Xu, B. *Nano Lett.* **2003**, *3*, 1261–1263.
20. Buzea, C. Pacheo, I. Robbie, K.. *Biointerphases*. **2007**, *2*, 2815690-2815745.
21. Nair, L. S. Laurencin, C. T. *J Biomed Nanotechnol.* **2007**, *3*, 301–316.
22. Ahamed, M. Karns, M. Goodson, M. Rowe, J. Hussain, S. M. Schlager, J. J. Hong, Y. *DNA Toxicol Appl Pharmacol* **2008**, *233*, 404–410.
23. Norman, R. S. Stone, J. W. Gole, A. Murphy, C. J. Sabo, A. T. L. *Nano Lett.* **2008**, *8*, 302-306.
24. Cheng, C. M. M. Cuda, G. Bunimovich, L. Y. Gaspari, M. Heath, R. J. Hill, D. H. Mirkin, A. C. Nijdam, J. A. Terracciano, R. Thundat, T. Ferrari, M. *Curr Opin Chem Biol.* **2006**, *10*, 11-19.
25. Hu, M. Chen, J. Li, Z. Y. Au, L. Hartland, G.V. Li, X. Marqueze, M. Xia, Y. Gold Nanostructures: Engineering their Plasmonic Properties for Biomedical Applications. *Chem Soc Rev.* **2006**, *35*, 1084-1094.
26. Shim, S. Y. Lim, D. K. Nam, J. M. *Nanomedicine.* **2008**, *3*, 215-232.
27. Huang, W. C. Tsai, P. J. Chen, Y.C. *Nanomedicine.* **2007**, *2*, 777-787.
28. Frens, G. *Nat Phys Sci.* **1973**, *241*, 20-22.
29. Ji, X. Song, X. Li, J. Bai, Y. Yang, W. Peng, X. *J Am Chem Soc.* **2007**, *129*, 13939–13948.

30. Kovtun, A. Heumann, R. Epple, M. *Biomed Mater Eng.* **2009**, *19*, 241–247.
31. Bunz, U. H. Rotello, V. M. *Angew Chem Int Ed.* **2010**, *49*, 3268–3279.
32. Wu, W. Li, A. D. *Nanomedicine.* **2007**, *2*, 523–531.
33. Liao, H. W. Nehl, C. L. Hafner, J. H. *Nanomedicine.* **2006**, *1*, 201-208.
34. Erathodiyil, N. Ying, J. Y. *Acc Chem Res.* **2011**, *44*, 925-935.
35. Kelly, L. K. Coronado, E. Zhao, L. Schatz, G. C. *J Phys Chem B.* **2003**, *107*, 668–677.
36. Auffan, M. Bottero, Y. J. Chaneac, C. Rose, J. *Nanomedicine.* **2010**, *5*, 999-1007.
37. Pal, S. Yu, K. T. Song, M. *J Appl Environ Microbiol.* **2007**, *73*, 1712–1720.
38. Badwaik, D.V. Bartonjojo, J. J. Evans, W. J. Sahi, V. S. Willis, B. C. Dakshinamurthy, R. *Langmuir.* **2011**, *27*, 5549-5554.
39. Daniel, M. C. Ruiz, J. Nlate, S. Blais, J. C. Astruc, D. *J Am Chem Soc.* **2003**, *125*, 2617–2628.
40. Leff, D. V. Ohara, P. C. Heath, J. R. Gelbart, W. M. *J Phys Chem.* **1995**, *99*, 7036–7041.
41. Chamundeeswari, M. Sobhana, L. S. S. Jacob, P. J. Kumar, G. M. Devi, P. M. Sastry, P. T. Mandal, B. A. *Biotechnol Appl Biochem* **2010**, *55*, 29-35.
42. Burygin, L. G. Khlebtsov, N. B. Shantrokha, N. A. Dykman, A. L. Bogatyrev, A. V. Khlebtsov, G.N. *Nanoscale Res Lett.* **2009**, *4*, 794-801.
43. Shrivastava, S. Bera, T. Roy, A. Singh, G. Ramachandrarao, P. Dash, D. *Nanotechnology.* **2007**, *18*, 225103-225112. Pandian, K.; Grace, N. A. *J Bionanoscience.* **2007**, *1*, 96-105.
44. Pandian, K.; Grace, N. A. *J Bionanoscience.* **2007**, *1*, 96-105.

45. Saha, B.; Bhattacharya, J.; Mukherjee, A.; Ghosh, K. A.; Santra, R. C.; Dasgupta, K. A.; Karmakar, P. *Nanoscale Res Lett.* **2007**, *2*, 614-622.
46. Santhana, R. L. Hing, H. L. Baharudin, O. The, H. Z. Aida, S. R. Nor, A. C. P. Vimala, B. Paramsarvaran, S. Sumarani, G. Hanjeet, K. *Annals of Microscope.* **2007**, *7*, 102-108.
47. Jung, K. W. Koo, C. H. Kim, W. K. Shin, S. Kim, H. S. Park, H. Y. *Appl Environ Microbiol.* **2008**, *74*, 2171-2178.
48. Robert, D. S. Robert, L. H. Martha, V. *J Bio. Chem.* **1908**, *5*, 485-487.
49. Vernon, L. P. Edward, S. W. *J Biol Chem.* **1927**, *74*, 379-383.
50. Vaara, M. *Microbiol Rev.* **1992**, *56*, 395-411.
51. Kadurugamuwa, J. L. Clarke, A. J. Beveridge, T. J. *J Bacteriology.* **1993**, *175*, 5798-5805.
52. Lowy, D. F. *Staphylococcus aureus* infections. *N Engl J Med.* **1998**, *339*, 520-532.
53. Ryan, K. J. Ray, C. G. *Medical Microbiology*, **2004**, *4*, 345-347.
54. Ndeke, M. Melusi, T. Nomakhwezi, N. *J Enviorn monitoring.* **2011**, *13*, 1164-1183.

